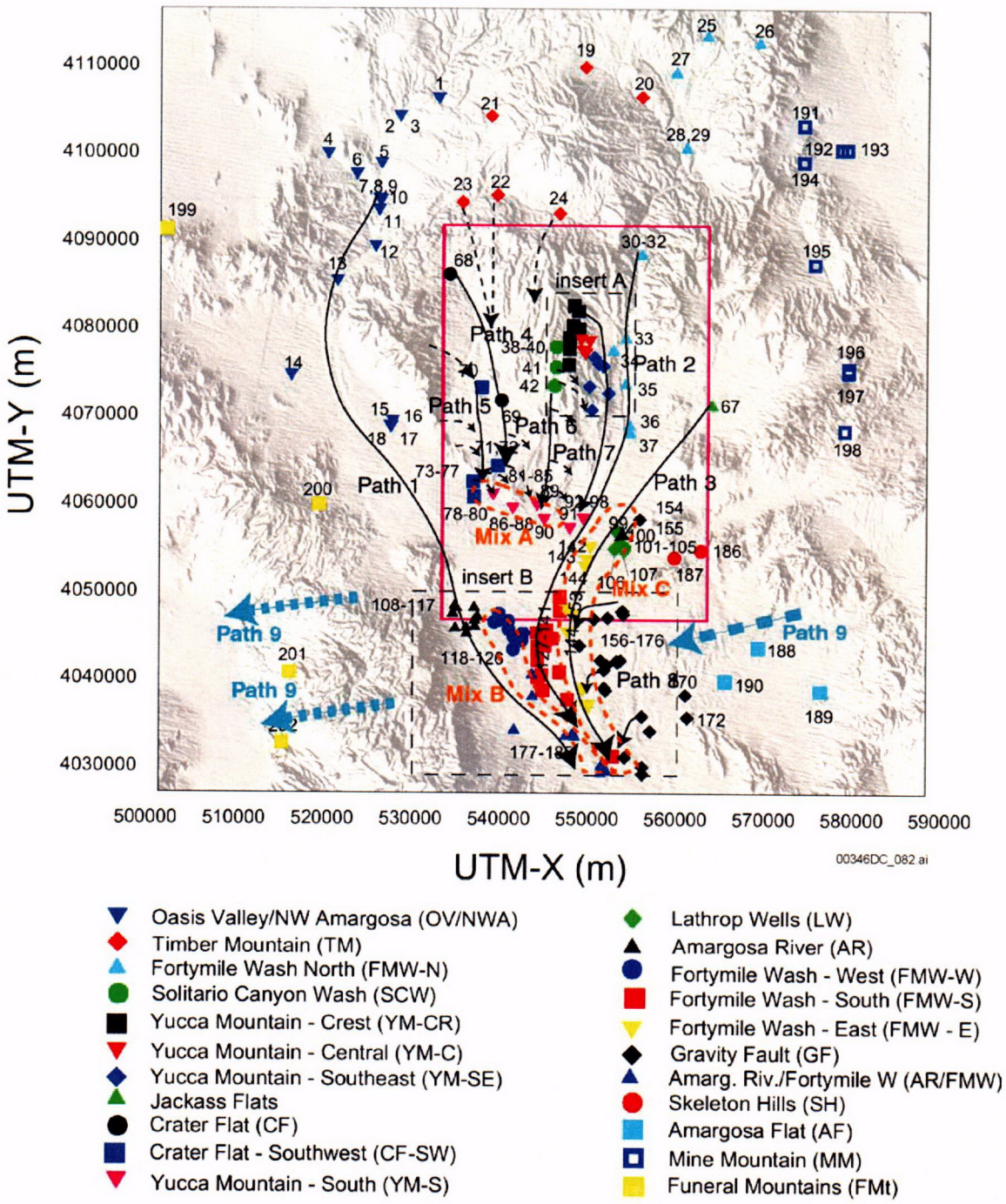

Source: BSC 2003c, Figure 62.

NOTE: The termination of flow paths implies that flow paths could not be traced from geochemical information downgradient from these areas because of mixing or dilution by more actively flowing groundwater; flow path terminations do not imply that groundwater stopped flowing.

Figure D-9. Geochemical Groundwater Types and Regional Flow Paths Inferred from Hydrochemical and Isotopic Data

A comparison of the predicted and observed geochemical flow paths indicates that the predicted flow paths generally correspond well with those identified through geochemical analysis. The generally good agreement between the two sets of flow paths qualitatively supports validation of the SSFM, particularly in demonstrating the capability of the SSFM to accurately simulate flow paths from the repository to the 5, 18, and 30-km boundaries.

Thermal Modeling–Measurements of temperature in the saturated zone constitute an independent data set that was not used in the calibration of the SSFM, but which can be used in validating the model. The transport of heat in the geosphere occurs generally upward toward the land surface, leading to lower temperatures near the surface. Heat is transported with groundwater in the saturated zone and can be used as a tracer for the movement of groundwater. To evaluate heat transport, modeling of heat transport through conduction only and through conduction with convective transport was undertaken. Heat distributions predicted by the conduction-only model and the coupled conduction with convective transport model were compared to evaluate the SSFM.

Data from temperature profiles measured in boreholes were used. Temperatures were extracted at 200-m intervals from the temperature profiles, and 94 observations from 35 boreholes were obtained (BSC 2003a, Section 7.4.2).

The SSFM was used as the basis for the conduction-only thermal model. The model domain and definitions of the hydrogeologic units are retained from the SSFM. Values of thermal conductivity were designated for each hydrogeologic unit. Values of thermal conductivity for the hydrogeologic units in the conduction-only thermal model were taken from a variety of literature sources (e.g., Sass et al. 1984; Brodsky et al. 1997; and Wollensber et al. 1983). The lateral boundaries of the conduction-only thermal model are set to no thermal flow, representing the essentially vertical transport of heat in the subsurface. The upper boundary condition was specified as a temperature-dependent heat flux in which the heat flux to the land surface was calculated as a function of the simulated temperature at the water table and the specified temperature at the land surface. The average annual temperature was based on the land surface elevation and varied by as much as 22°C over the model domain. A thermal conductance parameter was established to account for the thickness of the unsaturated zone. The bottom boundary was specified to represent upward heat transport from the deeper crust. The heat flux was assumed to be uniform because insufficient information was available to justify establishing a spatially variable heat flux at the bottom of the model.

The conduction-only thermal model was calibrated by adjusting the upper and lower thermal boundary conditions using a trial-and-error method. The conduction-only thermal model was run to steady-state thermal conditions. Observed and predicted temperatures were compared in a cross plot, and the calibration process sought to minimize the coefficient of determination (R^2) for this cross plot.

The best calibration of the conduction-only thermal model was obtained with a uniform heat flux of 35 mW/m^2 at the lower boundary and an equivalent thermal conductivity of 0.3 W/mK for the unsaturated zone at the upper boundary. The calibrated heat flux value at the lower boundary (35 mW/m^2) was lower than previously estimated by Sass et al. (1988), but it was within the estimated range of error (40 ± 9 mW/m^2) from that study. The calibrated thermal conductivity

value for the unsaturated zone was low relative to units in the saturated zone (0.3 W/mK versus about 1.4 to 1.7 W/mK for the volcanic formation of the Crater Flat tuff). However, this low thermal conductivity value also accounts for the effects of unsaturated conditions, stratification and variations in rock type, and percolation of groundwater.

Simulated temperatures at the water table for the calibrated conduction-only thermal model are shown in Figure D-10. There was considerable variation in the simulated temperature at the water table, primarily as a function of the unsaturated zone thickness. Higher simulated temperatures corresponded to the relatively thick unsaturated zone under Yucca Mountain and the Calico Hills (northeast corner of the model domain). Lower simulated temperatures occured in areas where the water table is closer to the land surface (southern part of the model domain and under Fortymile Canyon in the north). The pattern of simulated temperatures is influenced to a lesser extent by refraction of heat flow in the lower carbonate aquifer with its higher thermal conductivity.

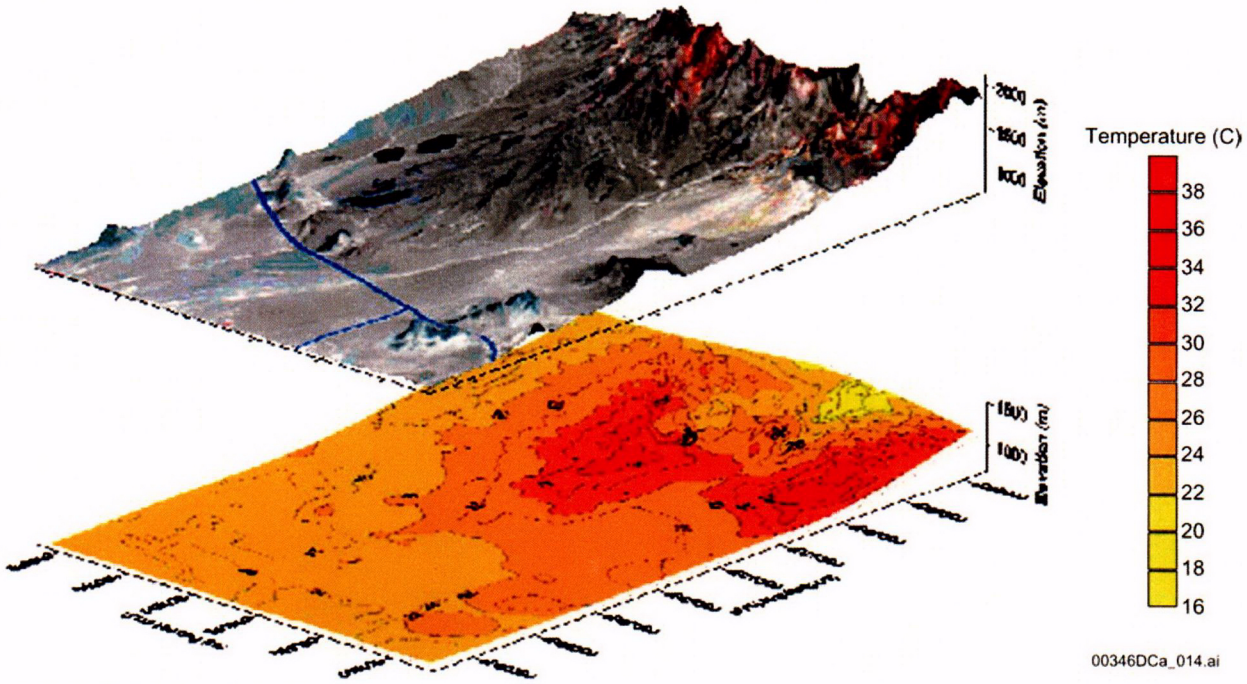

Source: BSC 2003a, Figure 7.4-3.

NOTE: Simulated temperature values are projected onto the water-table surface; the topographic surface (based on satellite imagery; color does not imply temperature) also is shown. The dark blue lines on the land surface are highways.

Figure D-10. Simulated Temperatures at the Water Table for the Conduction-Only Thermal Model

Residuals (Figure D-11) were determined for the 94 temperature data points, which generally were small (R^2 = 0.80). However, there was a tendency for the calibrated conduction-only thermal model to underestimate temperatures between 20°C and 35°C, to overestimate temperatures between 35°C and 50°C, and to underestimate temperatures over 50°C.

The spatial distribution of residuals at the water table indicated a systematic pattern (Figure D-11). Positive residuals tended to occur near and to the east of Yucca Mountain, whereas negative residuals tended to occur to the north and south of Yucca Mountain. Positive residuals indicate that simulated temperatures at the water table were too high.

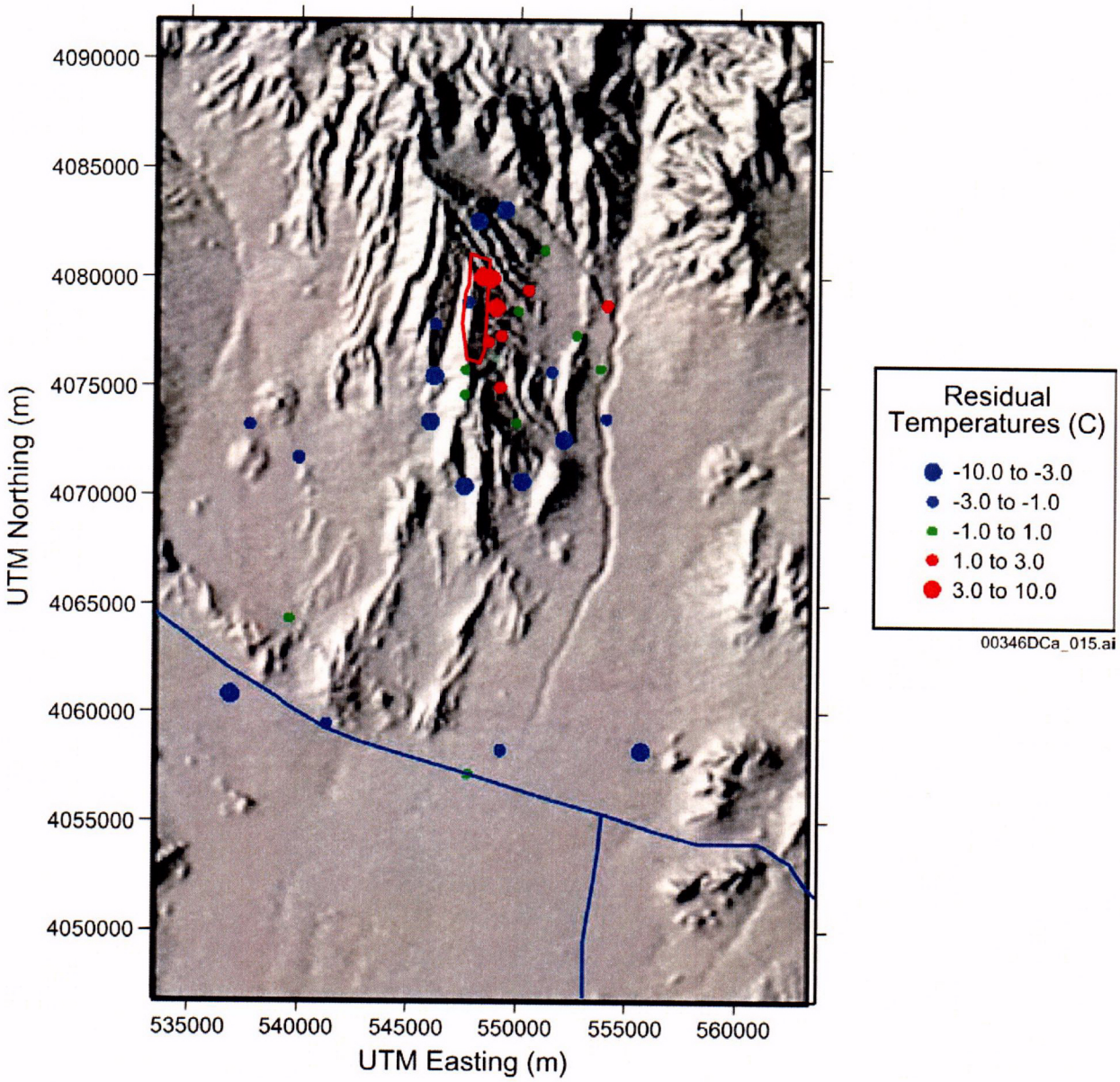

Source: BSC 2003a, Figure 7.4-6.

NOTE: Blue lines are highways.

Figure D-11. Residuals of Simulated Temperature at the Water Table for the Conduction-Only Thermal Model

Thermal modeling of groundwater flow and heat transport (coupled thermal modeling) provides a more complete representation of thermal transport processes in the saturated zone than does conduction-only modeling because groundwater flow redistributes heat laterally and vertically. In addition, variations in the density and viscosity of groundwater (a function of temperature) influence the groundwater flow field.

The SSFM and the conduction-only thermal model were used as the basis for the coupled thermal model. The calibrated upper and lower thermal boundary conditions from the conduction-only thermal model were used in the coupled thermal model. The temperature of groundwater flowing into the coupled thermal model at the lateral boundaries was specified to be equal to the simulated temperatures at those nodes in the conduction-only thermal model. Similarly, the specified groundwater flux from recharge on the upper boundary of the coupled thermal model was specified to be the simulated temperatures from the conduction-only thermal model.

The coupled thermal model was run to steady-state thermal and flow conditions for comparison with observed borehole temperatures. Joint calibration of the coupled thermal model to water-level and temperature measurements was not possible given the long computer run-times necessary to achieve a steady-state solution. Ideally, joint calibration of the SSFM using measured temperature and water-level data would provide explicit constraints on the groundwater flow field. Nonetheless, the uncalibrated, coupled thermal model can provide independent validation of the SSFM and subjective indications for improving it. The coupled thermal model constitutes an independent validation of the SSFM because it uses a data set that was not used in the calibration of the SSFM (i.e., temperatures in wells), adds the process of heat transport associated with temperature to the flow model, and adequately matches the temperature observations without altering the simulated flow conditions.

The resulting steady-state, simulated temperatures at the water table for coupled thermal model are shown in Figure D-12. Simulated temperatures at the water table for the coupled thermal model differ from the conduction-only thermal model in the area east of Yucca Mountain and in a small area in Crater Flat. The simulated temperatures generally were higher in the area between Yucca Mountain and Fortymile Wash in the coupled thermal model, indicating upward vertical advective heat transfer in this area. The small area of higher simulated temperatures in Crater Flat indicates another area of simulated upward groundwater flow.

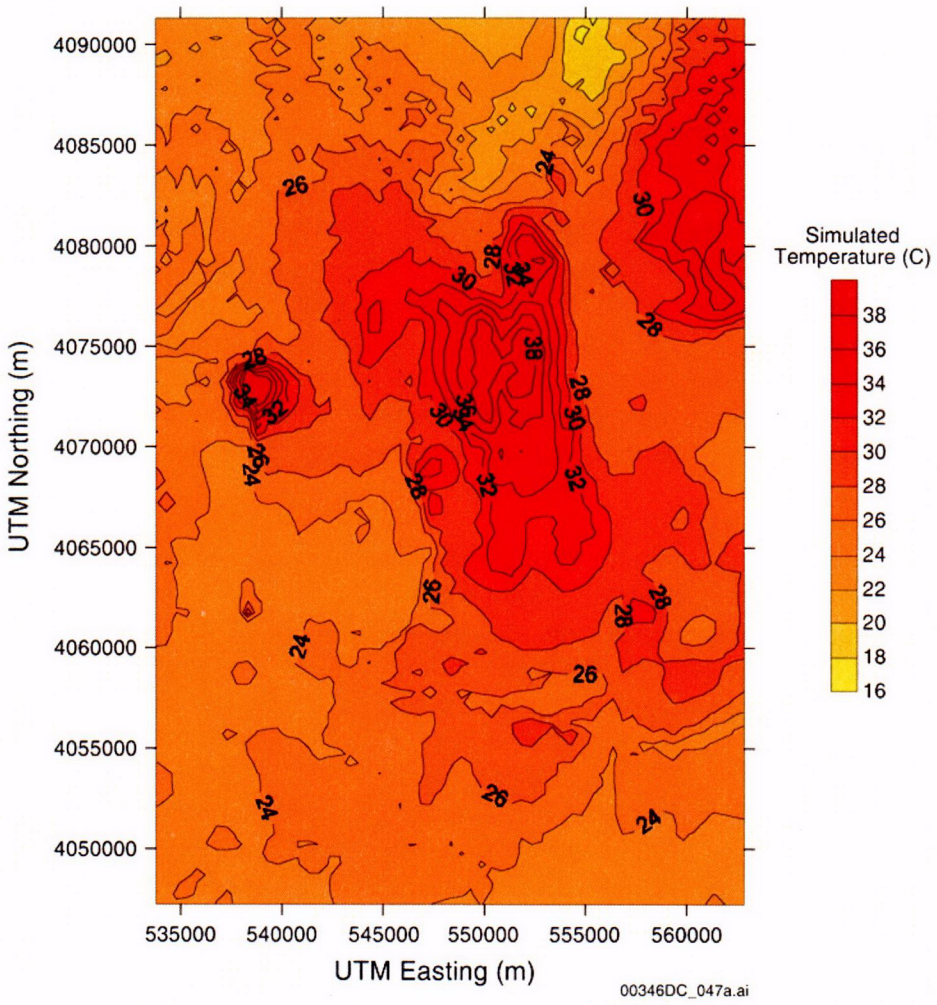

Source: BSC 2003a, Figure 7.4-7.

Figure D-12. Simulated Temperatures at the Water Table for the Coupled Thermal Model

Combining the calibrated SSFM and the calibrated coupled thermal model reduced the R^2 between observed and simulated temperatures from 0.80 to 0.62. However, the simulated temperatures for the deeper, higher-temperature measurement locations had positive and negative residuals from the coupled thermal model, whereas, the conduction-only thermal model consistently underestimated temperatures at these locations. The range of the statistical distribution of residuals for the coupled thermal model was more than the conduction-only thermal model, with an average of -0.13°C.

The spatial distribution of residuals in simulated temperature at the water table for the coupled thermal model is shown in Figure D-13. The largest positive residuals generally occur east and southeast of Yucca Mountain and in a relatively small area in Crater Flat. The largest negative residuals occur north of Yucca Mountain.

C12

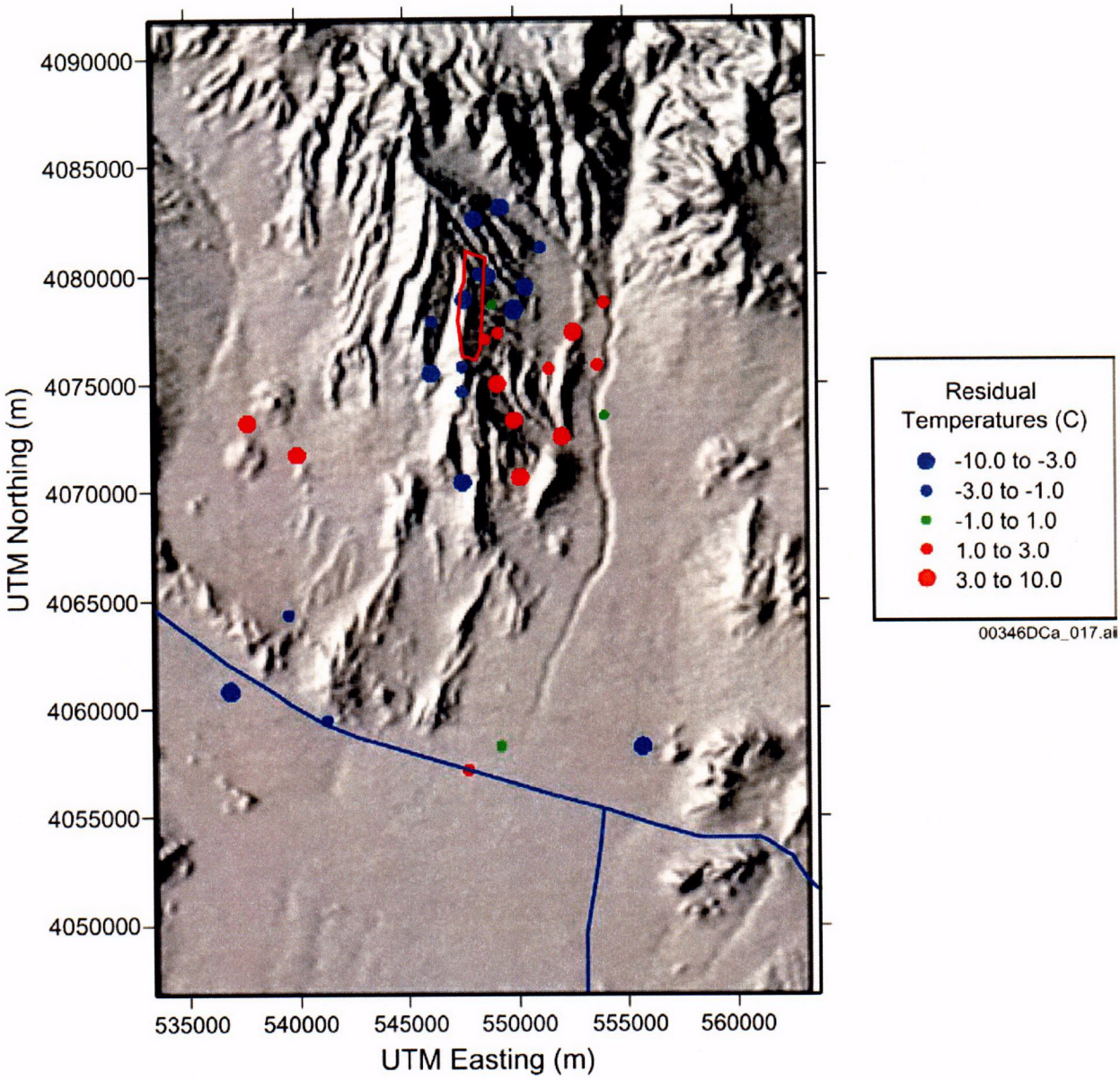

Source: BSC 2003a, Figure 7.4-9.

Figure D-13. Residuals in Simulated Temperature at the Water Table for the Coupled Thermal Model

Although a discernable spatial pattern in residuals was noted, the results of the coupled thermal model indicate that more than 90 percent of the simulated temperatures are within 10°C of the measured temperatures. Thus, the results of the coupled thermal model suggest an independent validation of the SSFM.

Comparison of Predicted Groundwater Velocity with Estimates from ATC Single-Borehole Tracer Tests–Three single-borehole injection-withdrawal tracer tests were conducted in borehole NC-EWDP-19D1 using nonsorbing solute tracers (BSC 2003b, Sections 6.3 and 6.5). The results of these tests were compared to determine the ambient groundwater velocity in the saturated alluvium south of Yucca Mountain. The primary difference between the three tests was that the tracers were allowed to "drift" for different periods of time (0, 2, and 30 days) before being pumped back out of the borehole. Four methods were used to estimate groundwater velocities. The first three methods involved between-test comparisons of the peak, mean, and late tracer arrival times, with the underlying assumption that differences in arrival times were due to the different times allowed for the movement of tracer plumes. The three methods assumed a confined aquifer, with the tracer mass corresponding to the arrival times assumed to be injected directly upgradient or downgradient from the borehole. The resulting groundwater velocity estimates depended on the assumed flow porosity. The fourth estimation method assumed a homogeneous, isotropic, confined aquifer. Although these assumptions are difficult to support, they allowed for estimating longitudinal dispersion and flow porosity from the single-borehole tracer tests, in addition to groundwater velocity. Assuming that the true flow porosity in the alluvium is between 0.05 and 0.30, groundwater velocity estimates from the first three methods ranged from 10 to 77 m/yr. The lower value was for the peak arrival analysis and an assumed flow porosity of 0.30, and the higher value was for the late arrival analysis and a flow porosity of 0.05. The fourth method yielded a groundwater velocity estimate of 15 m/yr, with a flow porosity of 0.10 and a longitudinal tracer dispersivity of 5 m. The specific discharge estimates from all four methods ranged from 1.2 to 9.4 m/yr. Additional groundwater velocity estimates, based on ^{14}C analyses, are presented in Appendix F.

Using the SSFM, specific discharge was estimated for a nominal fluid path leaving the proposed repository area and traveling 0 to 5 km, 5 to 20 km, and 20 to 30 km (BSC 2003a, Section 6.6.2.3). Specific discharge was determined for each segment of the flow path using the median travel time for a group of particles released beneath the repository. Specific discharge values of 0.67, 2.3, and 2.5 m/yr were obtained for the three segments, respectively. An expert elicitation panel (CRWMS M&O 1998, Figure 3-2e) estimated a median specific discharge of 0.71 m/yr for the 0 to 5-km segment (the panel did not consider other distances). The range of specific discharge estimates used in Yucca Mountain performance assessments is between 0.25 to 25 m/yr, with a most probable value being 2.5 m/yr. Thus, the range of specific discharge estimates from all four single borehole test methods is within the range used for the total system performance assessment.

D.4.3 Solitario Canyon Fault Alternate Conceptual Model (USFIC 5.11 AIN-1)

In the SSFM, the Solitario Canyon fault (Figure D-14) is represented as a fault with east and west branches at the southern end, each of which is considered to be a distinct feature with distinct hydrological properties. The Solitario Canyon fault consists of generally north-south trending features just west of Yucca Mountain. The two branches consist of generally north-northeast-trending linear features, also just west of Yucca Mountain. In the SSFM, the hydrological characteristics of these features enhance permeability in the vertical and fault-parallel directions, and they reduce permeability perpendicular to the faults.

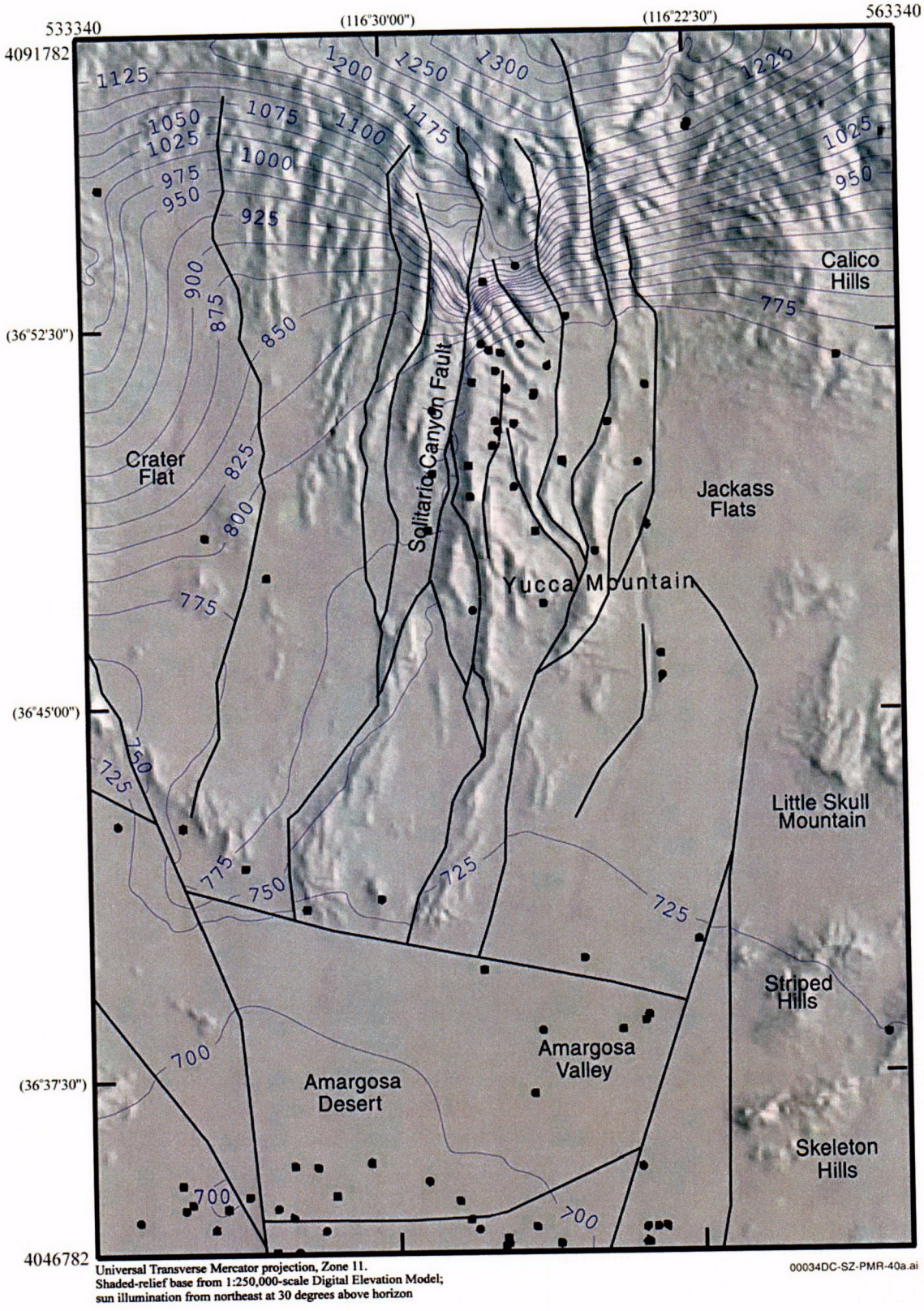

Source: Based on USGS 2001, Figure 1-2.

Figure D-14. Faults in the Yucca Mountain Region

C14

The parameterization of the Solitario Canyon fault is an important part of the SSFM because it can potentially control flow from Crater Flat to Fortymile Wash. The effect of these features on the SSFM is to generate a higher head gradient west of Yucca Mountain and to impede flow from Crater Flat to Yucca Mountain. This is important in determining the amount of alluvial material that groundwater flowing from beneath the repository passes through en route to the accessible environment. For the total system performance assessment for the site recommendation (CRWMS M&O 2000b), this fault was considered to extend from the bottom of the model domain to the top of the water table. However, conceptual uncertainty remains as to the depth of this fault. This uncertainty translates into uncertainty regarding the likely hydraulic behavior of this feature at depth.

To investigate the importance of the depth of the Solitario Canyon fault, an alternative conceptualization (shallow fault alternative model) was simulated in which the fault extended only from the water table to the top of the carbonate aquifer (BSC 2003a). The shallow fault alternative model was identical to the SSFM in all respects except for properties of the Solitario Canyon fault, and the only changes to the computation grid were those necessary to implement the alternate formulation of the fault. The shallow fault alternative model was calibrated in a manner identical to the SSFM.

The shallow fault alternative model was used to calculate head values for the 32 boreholes in the low-gradient region south and east of Yucca Mountain. These values were compared with measured values and values from the SSFM (BSC 2003a, Table 6.7-3). The shallow fault alternative model produced essentially the same results as the SSFM (i.e., with a deep Solitario Canyon fault). However, for the shallow fault alternative model, the calibrated permeability values were approximately 25 percent lower than the permeability values for the SSFM.

Groundwater flow paths from the SSFM and the shallow fault alternative model were evaluated using particle tracking. Two starting positions were considered: beneath Yucca Mountain and to the west of Yucca Mountain (west of the Solitario Canyon fault). Using the SSFM (deep Solitario Canyon fault), particle paths from beneath the repository generally were restricted to the upper few hundred meters of the saturated zone with some spreading to deeper paths in the alluvium south of Yucca Mountain (Figure D-15). Particle paths also were calculated from a source area near the water table to the west of the Solitario Canyon fault, and these generally were to the south and parallel to the Solitario Canyon fault for 5 and 10 km south of the repository, where flow paths crossed the southern branches of the Solitario Canyon fault from west to east (Figure D-16). Some flow paths crossed the branches of the Solitario Canyon fault at depths up to 1,500 m below the water table between 5 and 10 km south of the repository.

Using the shallow fault alternative model, particle paths from beneath the repository were similar to those from the SSFM (Figure D-17). Particle paths also were calculated from the source area west of the Solitario Canyon fault (Figure D-18). In map view, the flow paths are similar to those in the SSFM flow model; however, in cross-section, the flow paths that cross the southern branches of the Solitario Canyon fault did not extend to depths as great as those from the SSFM.

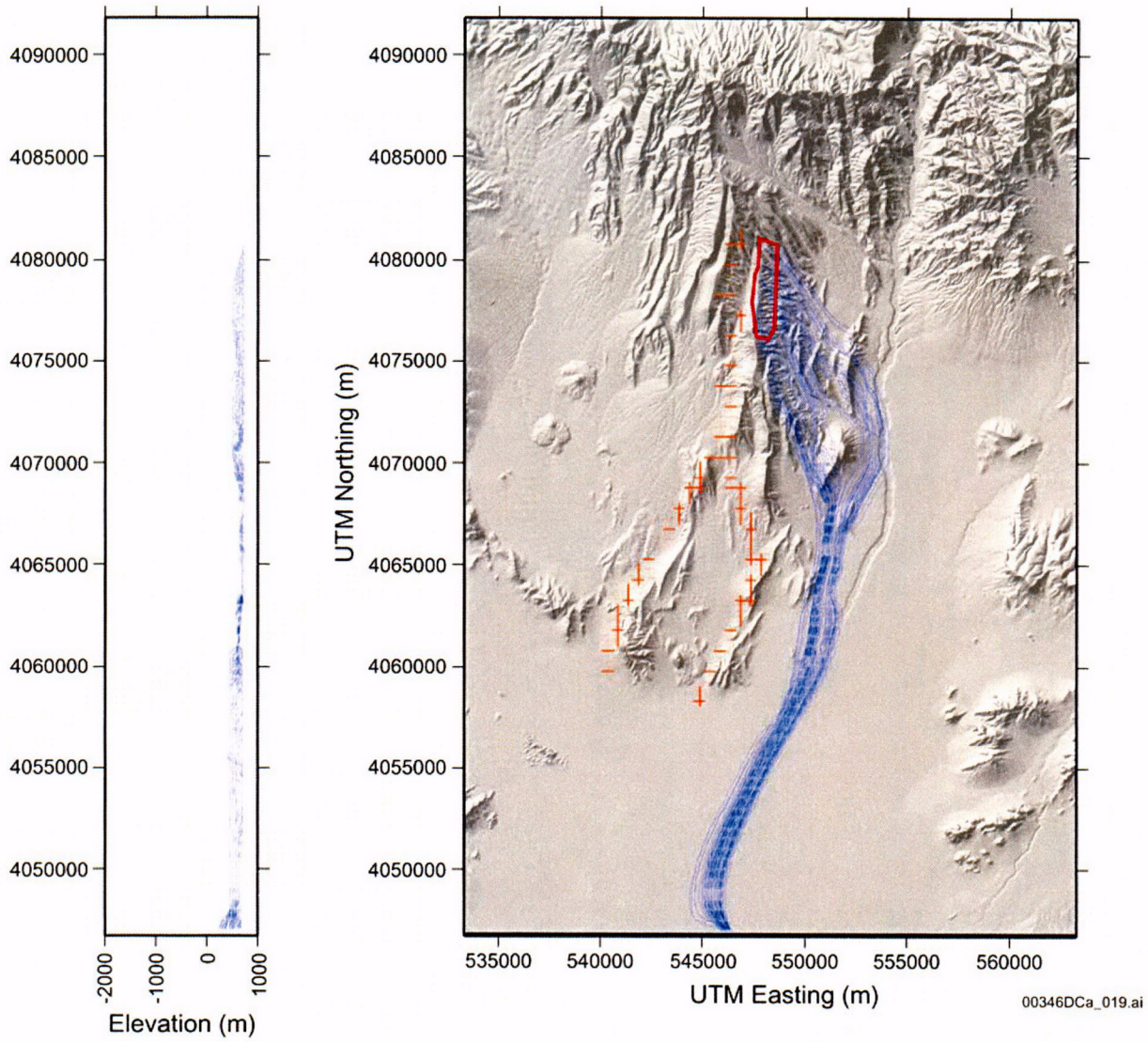

Source: BSC 2003a, Figure 6.7-5.

NOTE: Blue Lines–simulated flow paths; red line–repository outline; orange hatching–SSFM representation of the Solitario Canyon fault (Figure D-14).

Figure D-15. Simulated Groundwater Flow Paths Starting Beneath the Repository (SSFM using a Deep Solitario Canyon Fault)

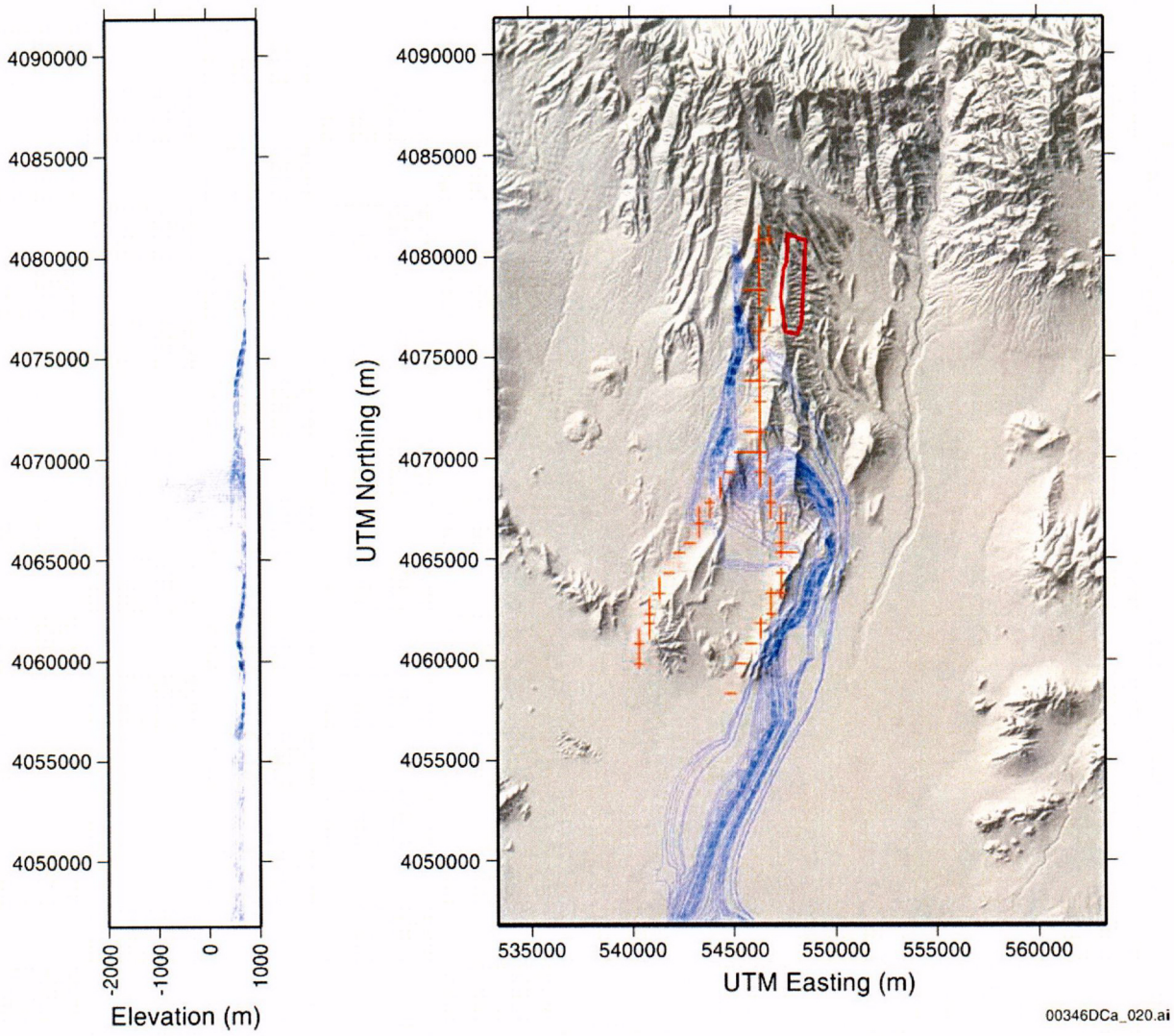

Source: BSC 2003a, Figure 6.7-6.

NOTE: Blue Lines—simulated flow paths; red line—repository outline; orange hatching—SSFM representation of the Solitario Canyon fault (Figure D-14). Particle paths start west of Solitario Canyon Fault, outside of the repository footprint, and do not represent the paths of radionuclides that may be released from the repository.

Figure D-16. Simulated Groundwater Flow Paths Starting West of Solitario Canyon (SSFM using a Deep Solitario Canyon Fault)

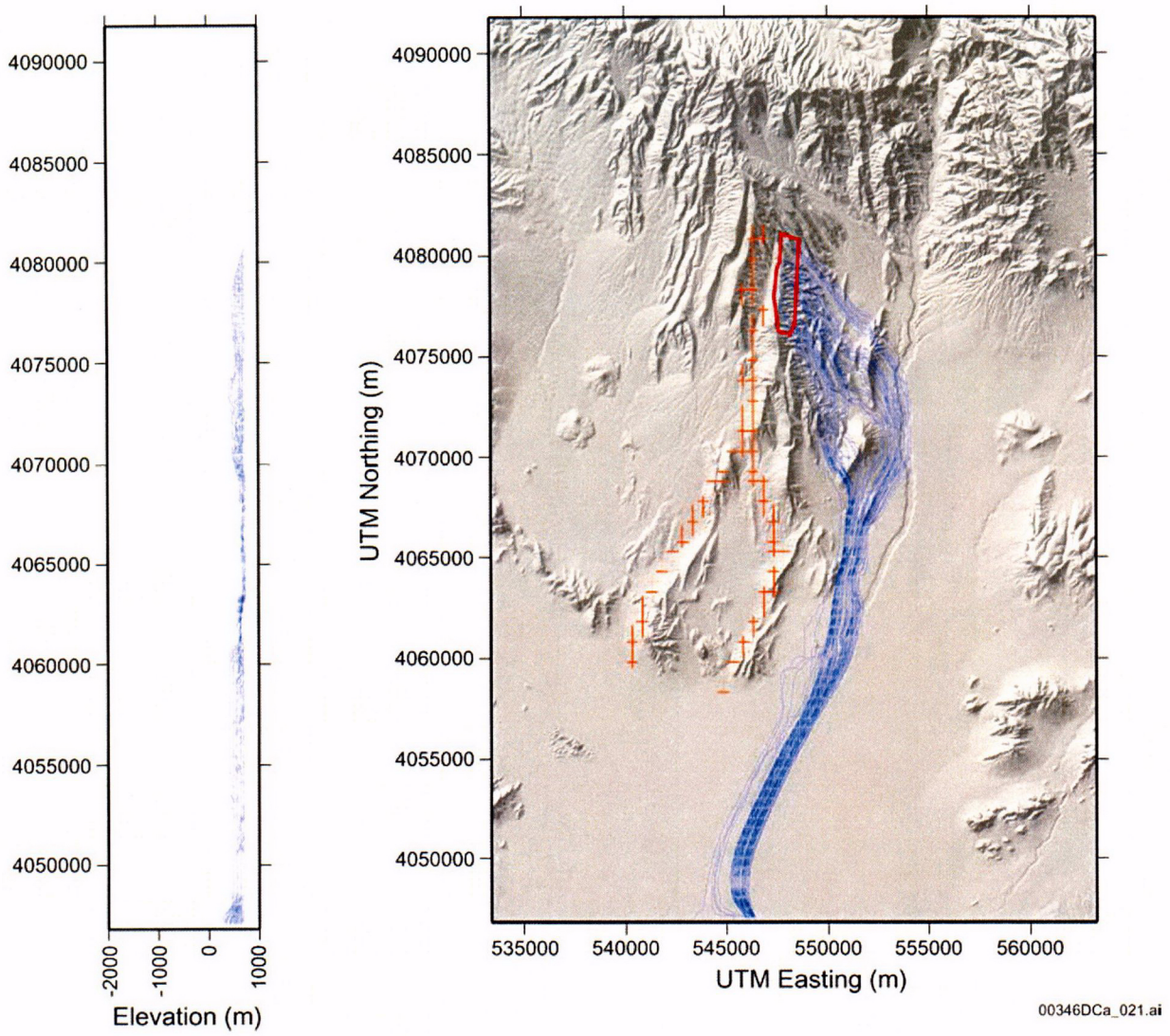

Source: BSC 2003a, Figure 6.7-7.

NOTE: Blue Lines–simulated flow paths; red line–repository outline; orange hatching–SSFM representation of the Solitario Canyon fault (Figure D-14).

Figure D-17. Simulated Groundwater Flow Paths Starting Beneath the Repository (Shallow Fault Alternative Model)

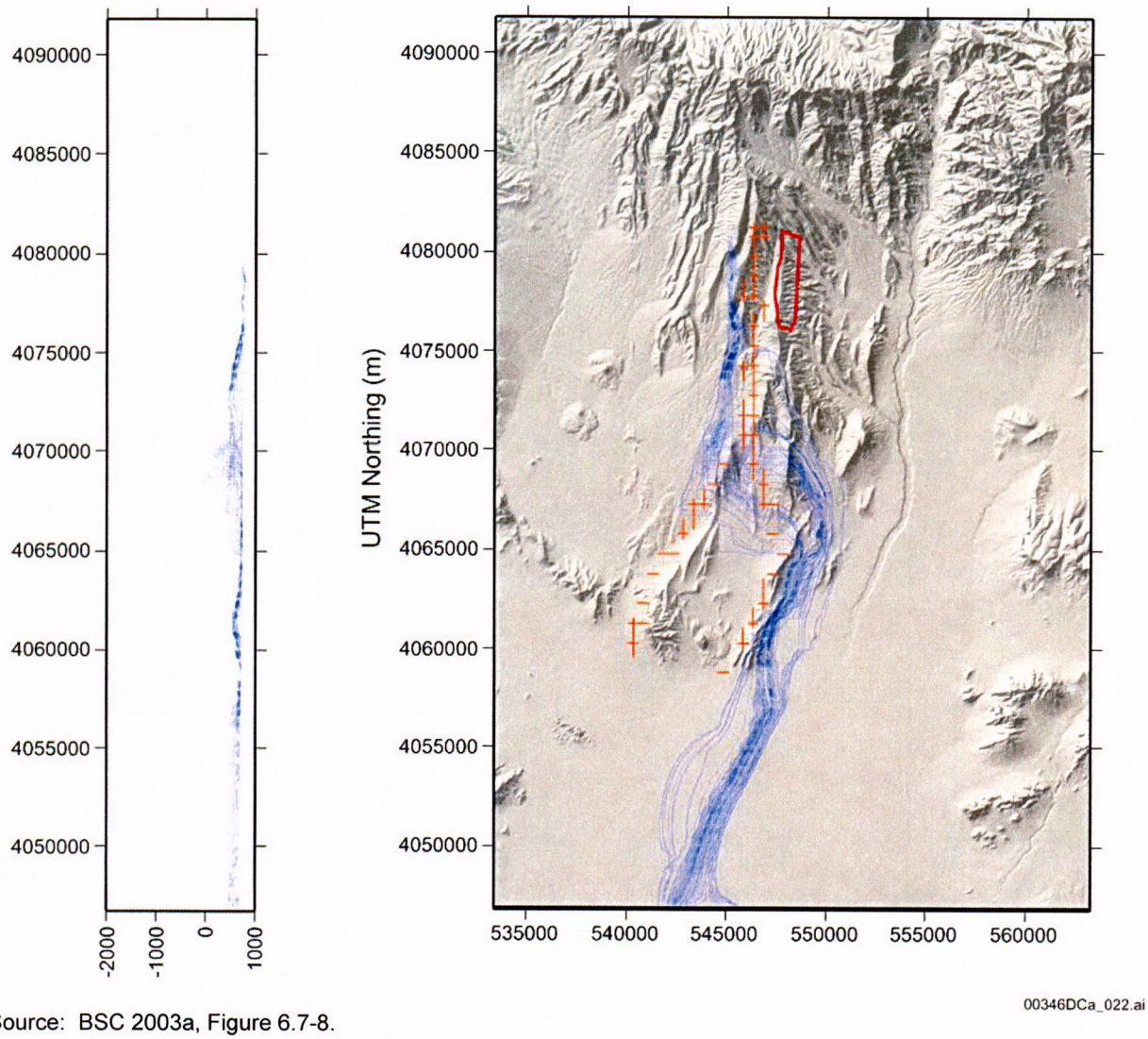

Source: BSC 2003a, Figure 6.7-8.

NOTE: Blue Lines–simulated flow paths; red line–repository outline; orange hatching–SSFM representation of the Solitario Canyon fault (Figure D-14). Particle paths start west of the Solitario Canyon fault, outside of the repository footprint, and do not represent the paths of radionuclides that may be released from the repository.

Figure D-18. Simulated Groundwater Flow Paths Starting West of Solitario Canyon (Shallow Fault Alternative Model)

Results of the Solitario Canyon fault simulations indicate that both conceptualizations produce essentially the same results. The simulated water levels, hydraulic gradients, and transport pathways were not greatly affected by the alternative conceptualization. The small differences in permeabilities and flow paths indicate that the depth of the Solitario Canyon fault did not affect travel times. Both conceptualizations yielded the same flow paths from the water table beneath the repository to the accessible environment, therefore travel times for the shallow-fault and deep-fault cases would be similar. The influence of reducing the depth of the Solitario Canyon fault on total system performance is expected to be minor. The alternative conceptualization of the Solitario Canyon fault, extending only from the water table to the top of the carbonate aquifer, resulted in slight changes to the flow system that were of no consequence for transport.

C18

D.5 REFERENCES

D.5.1 Documents Cited

Brodsky, N.S.; Riggins, M.; Connolly, J.; and Ricci, P. 1997. *Thermal Expansion, Thermal Conductivity, and Heat Capacity Measurements for Boreholes UE25 NRG-4, UE25 NRG-5, USW NRG-6, and USW NRG-7/7A.* SAND95-1955. Albuquerque, New Mexico: Sandia National Laboratories. ACC: MOL.19980311.0316.

BSC (Bechtel SAIC Company) 2001. *Calibration of the Site-Scale Saturated Zone Flow Model.* MDL-NBS-HS-000011 REV 00 ICN 01. Las Vegas, Nevada: Bechtel SAIC Company. ACC: MOL.20010713.0049.

BSC 2003a. *Site-Scale Saturated Zone Flow Model.* MDL-NBS-HS-000011 REV 01A. Las Vegas, Nevada: Bechtel SAIC Company. ACC: MOL.20030626.0296.

BSC 2003b. *Saturated Zone In-Situ Testing.* ANL-NBS-HS-000039 REV 00A. Las Vegas, Nevada: Bechtel SAIC Company. ACC: MOL.20030602.0291.

BSC 2003c. *Geochemical and Isotopic Constraints on Groundwater Flow Directions and Magnitudes, Mixing, and Recharge at Yucca Mountain.* ANL-NBS-HS-000021 REV 01A. Las Vegas, Nevada: Bechtel SAIC Company. ACC: MOL.20030604.0164.

CRWMS M&O (Civilian Radioactive Waste Management System Management and Operating Contractor) 1998. *Saturated Zone Flow and Transport Expert Elicitation Project.* Deliverable SL5X4AM3. Las Vegas, Nevada: CRWMS M&O. ACC: MOL.19980825.0008.

CRWMS M&O 2000a. *Saturated Zone Flow and Transport Process Model Report.* TDR-NBS-HS-000001 REV 00 ICN 02. Las Vegas, Nevada: CRWMS M&O. ACC: MOL.20001102.0067.

CRWMS M&O 2000b. *Total System Performance Assessment for the Site Recommendation.* TDR-WIS-PA-000001 REV 00 ICN 01. Las Vegas, Nevada: CRWMS M&O. ACC: MOL.20001220.0045.

D'Agnese, F.A.; Faunt, C.C.; Turner, A.K.; and Hill, M.C. 1997. *Hydrogeologic Evaluation and Numerical Simulation of the Death Valley Regional Ground-Water Flow System, Nevada and California.* Water-Resources Investigations Report 96-4300. Denver, Colorado: U.S. Geological Survey. ACC: MOL.19980306.0253.

D'Agnese, F.A.; O'Brien, G.M.; Faunt, C.C.; Belcher, W.R.; and San Juan, C. 2002. *A Three-Dimensional Numerical Model of Predevelopment Conditions in the Death Valley Regional Ground-Water Flow System, Nevada and California.* Water-Resources Investigations Report 02-4102. Denver, Colorado: U.S. Geological Survey. TIC: 253754.

Geldon, A.L.; Umari, A.M.A.; Fahy, M.F.; Earle, J.D.; Gemmell, J.M.; and Darnell, J. 1997. *Results of Hydraulic and Conservative Tracer Tests in Miocene Tuffaceous Rocks at the C-Hole Complex, 1995 to 1997, Yucca Mountain, Nye County, Nevada.* Milestone SP23PM3. [Las Vegas, Nevada]: U.S. Geological Survey. ACC: MOL.19980122.0412.

Reamer, C.W. and Williams, D.R. 2000. Summary Highlights of NRC/DOE Technical Exchange and Management Meeting on Unsaturated and Saturated Flow Under Isothermal Conditions. Washington, D.C.: U.S. Nuclear Regulatory Commission. ACC: MOL.20001128.0206.

Sass, J.H.; Kennelly, J.P., Jr.; Smith, E.P.; and Wendt, W.E. 1984. *Laboratory Line-Source Methods for the Measurement of Thermal Conductivity of Rocks Near Room Temperature.* Open-File Report 84-91. Menlo Park, California: U.S. Geological Survey. ACC: NNA.19920814.0125.

Sass, J.H.; Lachenbruch, A.H.; Dudley, W.W., Jr.; Priest, S.S.; and Munroe, R.J. 1988. *Temperature, Thermal Conductivity, and Heat Flow Near Yucca Mountain, Nevada: Some Tectonic and Hydrologic Implications.* Open-File Report 87-649. [Denver, Colorado]: U.S. Geological Survey. TIC: 203195.

Schlueter, J.R. 2003. "Additional Information needed for Unsaturated and Saturated Flow Under Isothermal Conditions (USFIC).5.11 Agreement and Completion of General (GEN).1.01, Comment 103." Letter from J.R. Schlueter (NRC) to J.D. Ziegler (DOE/ORD), February 5, 2003, 0210036017, with enclosure. ACC: MOL.20030805.0395.

USGS (U.S. Geological Survey) 2001. *Hydrogeologic Framework Model for the Saturated-Zone Site-Scale Flow and Transport Model.* ANL-NBS-HS-000033 REV 00 ICN 02. Denver, Colorado: U.S. Geological Survey. ACC: MOL.20011112.0070.

Wollenberg, H.A.; Wang, J.S.Y.; and Korbin, G. 1983. *An Appraisal of Nuclear Waste Isolation in the Vadose Zone in Arid and Semiarid Regions (with Emphasis on the Nevada Test Site).* LBL-15010. Berkeley, California: University of California, Lawrence Berkeley Laboratory. TIC: 211058.

Ziegler, J.D. 2002. "Transmittal of Report Addressing Key Technical Issue (KTI) Agreement Item Unsaturated and Saturated Zone Flow Under Isothermal Conditions (USFIC) 5.11." Letter from J.D. Ziegler (DOE/YMSCO) to J.R. Schlueter (NRC), July 5, 2002, 0709023235, OL&RC:TCG-1357, with enclosure. ACC: MOL.20020911.0130.

Ziegler, J.D. 2003. "Response to Additional Information Needed on Key Technical Issue (KTI) Agreement Item Unsaturated and Saturated Flow Under Isothermal Conditions (USFIC) 5.11." Letter from J.D. Ziegler (DOE/ORD) to J.R. Schlueter (NRC), April 9, 2003, 0410036845, OLA&S:TCG-0976. ACC: MOL.20030529.0290.

D.5.2 Data, Listed by Data Tracking Number

MO0105GSC01040.000. Survey Of Nye County Early Warning Drilling Program (EWDP) Phase I Borehole NC-EWDP-09S. Submittal date: 05/15/2001.

MO0106GSC01043.000. Survey Of Nye County Early Warning Drilling Program (EWDP) Phase II Boreholes. Submittal date: 06/13/2001.

MO0203GSC02034.000. As-Built Survey Of Nye County Early Warning Drilling Program (EWDP) Phase III Boreholes NC-EWDP-10S, NC-EWDP-18P, AND -C-EWDP-22S - Partial Phase III List. Submittal date: 03/21/2002.

MO0206GSC02074.000. As-Built Survey Of Nye County Early Warning Drilling Program (EWDP) Phase III Boreholes, Second Set. Submittal date: 06/03/2002.

D.5.3 Codes, Standards, Regulations, and Procedures

AP-SIII.10Q, Rev. 1, ICN 0. *Models.* Washington, D.C.: U.S. Department of Energy, Office of Civilian Radioactive Waste Management. ACC: DOC.20030312.0039.

INTENTIONALLY LEFT BLANK